J. Biochem. 2012;152(2):133–138 doi:10.1093/jb/mvs070

JB THE JOURNAL OF BIOCHEMISTRY

The *in silico* screening and X-ray structure analysis of the inhibitor complex of *Plasmodium falciparum* orotidine 5′-monophosphate decarboxylase

Received September 23, 2011; accepted January 12, 2012; published online June 26, 2012

Yasuhide Takashima[1], Eiichi Mizohata[1], Sudaratana R. Krungkrai[2], Yoshifumi Fukunishi[3], Takayoshi Kinoshita[4], Tsuneaki Sakata[5], Hiroyoshi Matsumura[1], Jerapan Krungkrai[6], Toshihiro Horii[7] and Tsuyoshi Inoue[1,*]

[1]Department of Applied Chemistry, Graduate School of Engineering, Osaka University, 2-1 Yamadaoka, Suita, Osaka 565-0871, Japan; [2]Unit of Biochemistry, Department of Medical Science, Faculty of Science, Rangsit University, Patumthani 12000, Japan; [3]National Institute of Advanced Industrial Science and Technology (AIST), 2-3-26, Aomi, Koto-ku, Tokyo 135-0064, Japan; [4]Department of Applied Biochemistry, Graduate School of Agriculture and Life Sciences, Osaka Prefecture University, 1-1 Gakuen-cho, Sakai, Osaka 599-8531, Japan; [5]Cybermedia Center, Osaka Univ. 5-1 Mihogaoka, Ibaraki, Osaka 567-0047, Japan; [6]Department of Biochemistry, Faculty of Medicine, Chulalongkorn University, Rama IV Road, Bangkok 10330, Thailand; and [7]Department of Molecular Protozoology, Research Institute for Microbial Diseases, Osaka University, 3-1 Yamadaoka, Suita, Osaka 565-0871, Japan

*Dr. Tsuyoshi Inoue, Department of Molecular Protozoology, Research Institute for Microbial Diseases, Osaka University, 3-1 Yamadaoka, Suita, Osaka 565-0871, Japan. Tel: +81-6-6879-7408, Fax: +81-6-6879-7409, email: inouet@chem.eng.osaka-u.ac.jp

Orotidine 5′-monophosphate decarboxylase from *Plasmodium falciparum* (*Pf*OMPDC) catalyses the final step in the *de novo* synthesis of uridine 5′-monophosphate (UMP) from orotidine 5′-monophosphate (OMP). A defective *Pf*OMPDC enzyme is lethal to the parasite. Novel *in silico* screening methods were performed to select 14 inhibitors against *Pf*OMPDC, with a high hit rate of 9%. X-ray structure analysis of *Pf*OMPDC in complex with one of the inhibitors, 4-(2-hydroxy-4-methoxyphenyl)-4-oxobutanoic acid, was carried out to at 2.1 Å resolution. The crystal structure revealed that the inhibitor molecule occupied a part of the active site that overlaps with the phosphate-binding region in the OMP- or UMP-bound complexes. Space occupied by the pyrimidine and ribose rings of OMP or UMP was not occupied by this inhibitor. The carboxyl group of the inhibitor caused a dramatic movement of the L1 and L2 loops that play a role in the recognition of the substrate and product molecules. Combining part of the inhibitor molecule with moieties of the pyrimidine and ribose rings of OMP and UMP represents a suitable avenue for further development of anti-malarial drugs.

Keywords: inhibitor complex/*in silico* screening/malaria/orotidine 5′-monophosphate decarboxylase/X-ray structure analysis.

Abbreviations: DSI, docking score index; DTT, dithiothreitol; HMOA, 4-(2-hydroxy-4-methoxyphenyl)-4-oxobutanoic acid; MTS, multiple target screening; OMPDC, orotidine 5′-monophosphate decarboxylase; OMP, orotidine 5′-monophosphate; PfOMPDC, orotidine 5′-monophosphate decarboxylase from *Plasmodium falciparum*; UMP, uridine 5′-monophosphate.

There are an estimated 300–500 million cases of malaria, and up to three million people die of this disease annually. *Plasmodium falciparum* is the causative agent of the most lethal and severe form of human malaria (*1*). The chemotherapy for the treatment of malaria is available but is complicated by both adverse side-effects and widespread resistance to most of the currently available anti-malarial drugs (*2*, *3*). Thus, more efficacious and less toxic agents that specifically target the parasite are required.

The malaria parasite depends on *de novo* synthesis (Supplementary Fig. 1) of pyrimidine nucleotides, whereas humans can synthesize these nucleotides by both *de novo* and salvage pathways (*4–6*). The final two steps of uridine 5′-monophosphate (UMP) synthesis require the addition of ribose 5-phosphate from 5-phosphoribosyl-1-pyrophosphate to orotic acid by orotate phosphoribosyltransferase (EC 2.4.2.10) to form orotidine 5′-monophosphate (OMP). Subsequently, decarboxylation of OMP by OMP decarboxylase (OMPDC; EC 4.1.1.23) forms UMP. In most prokaryotes and in the malaria parasite, both the enzymes are encoded by two separate genes (*7*, *8*). Our previous studies demonstrated that the two enzymes exist as a heterotetrameric (orotate phosphoribosyltransferase)$_2$(OMPDC)$_2$ complex in two species of malaria, *P. falciparum* and *Plasmodium berghei* (*9*, *10*). In contrast, these genes found in most multicellular organisms, including humans, are fused as a single gene, resulting in the bifunctional UMP synthase (*11–13*).

One of the most important problems associated with *in silico* screening methods is the prediction of the structures of the protein-ligand complexes. The standard approach involves selecting a chemical compound as a drug candidate based on docking scores. However, the hit rate is usually low *in vivo* and *in vitro*. In some cases, particular chemical compounds that have high

docking scores for a target protein also display relatively high scores for other proteins, thereby reducing the selectively for the target protein. Fukunishi and Nakamura have developed a multiple target screening (MTS) (*14*) method that uses a matrix of ΔG containing several million compounds and several hundred protein structures to select the candidates that most strongly interact with the target protein among the protein list in the matrix. Moreover, the docking score index (DSI) (*15*) method was developed as a method for screening similar compounds, using the matrix-like MTS method.

In this study, 14 inhibitors for *Pf*OMPDC were selected using the novel *in silico* screening methods. The crystal structure of *Pf*OMPDC in complex with one of the inhibitors, 4-(2-hydroxy-4-methoxyphenyl)-4-oxobutanoic acid (HMOA), was solved at 2.1 Å resolution. We relate the large structural changes of the loops to the recognition of the substrate or product molecules, and thus provide structural insights for further development of an effective inhibitor.

Materials and Methods

Expression and purification of PfOMPDC

Orotidine 5′-monophosphate decarboxylase from *Plasmodium falciparum* (*Pf*OMPDC) was expressed in *Escherichia coli* BL21(DE3)pLysS (Novagen) as previously described (*16*). The *E. coli* cells were disrupted by sonication with 5 mM Tris-HCl buffer (pH 8.0) containing 50 mM NaCl, 1 mM imidazole and a protease inhibitor cocktail (Roche). The sample was applied to a Ni^{2+}-loaded HiTrap chelating HP (GE Healthcare) column equilibrated with buffer A (50 mM Tris-HCl [pH 8.0], 500 mM NaCl and 10 mM imidazole). His-tagged proteins were eluted with a 10–500 mM imidazole linear gradient in buffer A. The fractions containing *Pf*OMPDC were pooled and applied to a HiLoad 16/60 Superdex 75 column (GE Healthcare), which was equilibrated with buffer B (50 mM Tris–HCl [pH 8.0], 300 mM NaCl and 5 mM dithiothreitol [DTT]). The purified protein was concentrated to 10 mg mL^{-1} using an ultracentrifugation concentrator (Sartorius) and was stored at 193 K until crystallization experiments. Up to 12 mg of purified *Pf*OMPDC was obtained from 9 L of the *E. coli* cell culture.

In silico screening

By using a one million compound library with molecular weights of <350 Da, the inhibitor candidates for *Pf*OMPDC were first selected using both the MTS (*14*) and DSI (*15*) methods. The structure of *Pf*OMPDC with the substrate OMP was used (PDB code 2ZA1) during the trial of *in silico* screening. Subsequently, the scoring function using the molecular mechanics Poisson–Boltzmann surface area method (*17*) was used to evaluate the docking results and to rank the ligand-binding affinities. 200 highest-scoring compounds were ordered as the candidates in total. (Namiki Shoji Co., Ltd.).

SPR analysis

All experiments were performed using an AP-3000 system (Label-free Affinity Perceptive System) (Fuji Photo Film Co. Ltd.). The solution of 0.1 mg mL^{-1} *Pf*OMPDC diluted in 10 mM sodium acetate buffer (pH 5.5) was immobilized onto the surface of a sensor stick through amine chemistry according to standard procedures. Briefly, a 50:50 solution of 0.1 M N-hydroxysuccinimide and 0.4 M 1-ethyl-3-(3-dimethylaminopropyl) carbodiimide hydrochloride was injected over the stick surface at 10 μL min^{-1} for 7 min. The sample solution was then flowed over the activated surface. The remaining activated sites were quenched by flowing 1 M ethanolamine and then washed once with 10 mM HEPES buffer (pH 7.4) over the chip surface at 5 μL sec^{-1} for 15 min. The two solutions were prepared in 10 mM HEPES buffer (pH 7.4) containing 250 μM DTT and 0.5 or 1.5% dimethyl sulfoxide. These solutions were used for calibration and were injected as the running buffer (10 mM HEPES [pH 7.4], 250 μM DTT and 1% dimethyl sulfoxide). Each compound was diluted in running buffer and applied in the range of 3.9–500 μM at 5 μL sec^{-1} for 15 min. The temperature was kept at 295 K.

IC_{50} assays for decarboxylation of PfOMPDC

An inhibition assay of candidate compounds for *Pf*OMPDC was performed as described previously (*9*). Briefly, the reaction mixture (1 mL) was prepared in 50 mM Tris–HCl buffer (pH 8.0) containing 250 μM DTT. The enzyme (5–50 μL) was incubated for 1 min at 310 K. The reaction was then started by the addition of 250 μM OMP and followed through a linear progress curve of absorbance change at 285 nm up to 3–6 min. The difference of the extinction coefficients at 285 nm between OMP and UMP was $1.65 \times 10^3\ M^{-1}\ cm^{-1}$ (*18*).

Data collection and processing

The crystal of *Pf*OMPDC in complex with the HMOA did not appear using previous crystallization conditions (*16*). A novel crystal of apo *Pf*OMPDC was grown by the hanging-drop vapor-diffusion method at 293 K within 1 day. A drop consisted of 1 μL of the protein solution (10 mg ml^{-1} *Pf*OMPDC, 50 mM Tris–HCl [pH 8.0], 300 mM NaCl and 5 mM DTT) with 1 μL of the reservoir solution (100 mM Tris-HCl [pH 8.0], 27% PEGmme 2K and 3% 1,6-hexandiol). To prepare the *Pf*OMPDC-HMOA complex, the crystal was soaked into an HMOA-containing cryoprotectant solution (100 mM Tris-HCl (pH 8.0), 27% PEGmme 2K, 20% glycerol, 3% 1,6-hexandiol and 3.3 μM HMOA) for 2 min.

X-ray diffraction data of the inhibitor complex were collected at the BL38B1 beamline (SPring-8, Japan). The crystal was mounted on a standard nylon loop in a stream of nitrogen at 100 K. The diffraction patterns were recorded on an ADSC Quantum 315 CCD detector. The diffraction intensity data were processed and scaled using *HKL2000* (*19*). The statistics of the diffraction data collection are shown in Table I.

Structure determination and refinement

The molecular replacement calculations were performed with the program *MOLREP* (*20*) in the *CCP4* program package (*21*), using the OMP-complex structure of *Pf*OMPDC (PDB code 2ZA1) as the search model. A dimer molecule was contained in an asymmetric unit of the crystal. The electron density map was improved by density modification and non-crystallographic symmetry averaging using *DM* (*22*). Structure models were refined against the diffraction data using *CNS* (*23*) and *REFMAC5* (*24*). Visualization of electron density and model building were performed using *Coot* (*25*).

Results and Discussion

Inhibitor search by in silico screening methods

To find novel anti-malarial drugs, 5,000 compounds from the one million compound library were screened using either the MTS (*14*) or DSI (*15*) methods, respectively. Among the 10,000 compounds screened, 2,378 were selected by both methods. As a result, 7,622 compounds were selected in total. The ligand-binding affinities between the protein and selected candidates were computed using the molecular mechanics Poisson–Boltzmann surface area (*17*) method. The highest scoring 200 compounds with $|\Delta G|$ values in the range of 20–130 kcal mol^{-1} were selected; 156 of these compounds could be obtained commercially (Fig. 1). The mean value and the standard deviation of the scores for the highest scoring 200 compounds were −23.7 and 3.1 kcal mol^{-1}, respectively. Although the compounds ranked from 3603 to 7622 had more than 0 kcal mol^{-1} of ΔG values, the values for the rest of compounds that ranked from 201 to 3602 were −8.4 and 5.1 kcal mol^{-1}, respectively. Of these 156 compounds, 43 exhibited the affinity for *Pf*OMPDC at ≤500 μM with SPR analyses. Finally, 14 inhibitors

Table I. Data collection and refinement statistics for *Pf*OMPDC in complex with HMOA.

Diffraction data	
Space group	*R*3
Cell dimensions (Å)	
	$a = b = 201.97$
	$c = 44.28$
Resolution (Å)	50–2.10 (2.14–2.10)
Measured reflection (n)	439,637
Unique reflection (n)	37,285
Completeness (%)	95.1 (88.7)
R_{merge}[a] (%)	6.2 (32.5)
Refinement statistics	
Resolution (Å)	50–2.10
R_{work}[b] (%)	21.2
R_{free}[c] (%)	28.6
No. of water molecules	144
Root mean square deviation bond length (Å)	0.019
Root mean square deviation bond angle (°)	1.825

Values in parentheses are for the highest resolution shell (2.14–2.10 Å).
[a] $R_{merge} = \sum_{hkl} \sum_i |I_i(hkl) - \langle I(hkl)\rangle| / \sum_{hkl} \sum_i I_i(hkl)$, where $I_i(hkl)$ is the *i*th intensity measurement and $\langle I(hkl)\rangle$ is the mean of all measurements of $I(hkl)$.
[b] $R_{work} = \sum_{hkl} ||F_{obs}| - |F_{calc}|| / \sum_{hkl} |F_{obs}|$ calculated from 95% of the data, which were used during the course of the refinement.
[c] $R_{free} = \sum_{hkl} ||F_{obs}| - |F_{calc}|| / \sum_{hkl} |F_{obs}|$ calculated from 5% of the data, which were used during the course of the refinement.

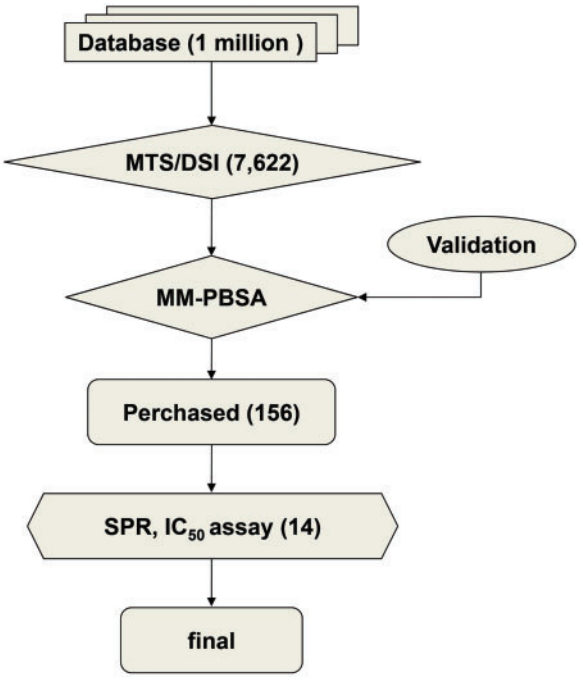

Fig. 1 Schematic representation of the strategy for *in silico* screening. The inhibitor candidates for *Pf*OMPDC were selected from a one million compound library using the MTS and DSI methods. The selected compounds were then measured by SPR analysis and IC_{50} assays.

were found to have potent competitive inhibition ≤250 μM as determined by IC_{50} assays (Fig. 2).

Generally, the hit rate of *in silico* screening is about 1–10%, which is higher than that of the high-throughput screening method (0.01%) (*26*). In the

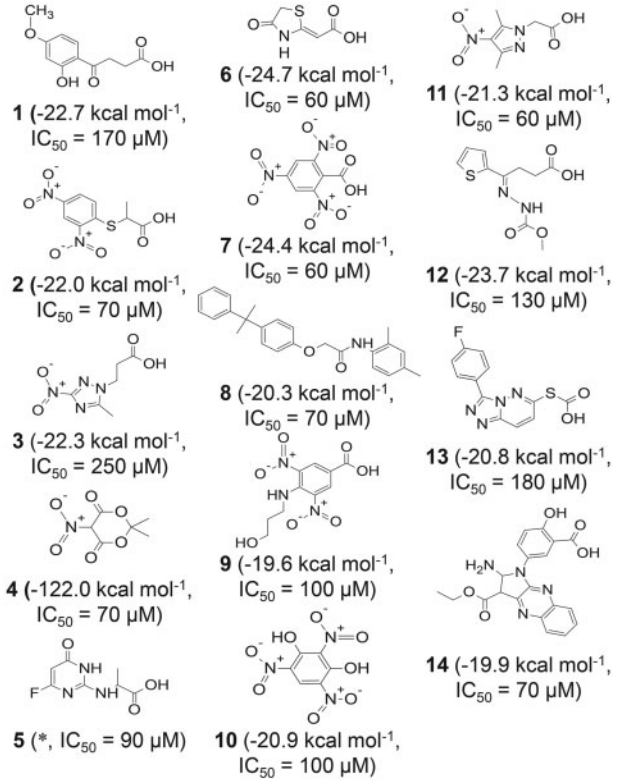

Fig. 2 Fourteen inhibitor candidates for *Pf*OMPDC. The scores for *in silico* screening and IC_{50} value for each compound were shown in brackets, respectively. The *Pf*OMPDC structure complexed with compound **1** was solved in this study. *The docking score is not shown because of the lack of the stable structure among the binding prediction (docking).

present study, 14 out of 156 purchased compounds were identified as inhibitor candidates for *Pf*OMPDC, giving a hit rate of 9%. Consequently, our *in silico* screening methods displayed a 1,000-fold higher hit rate when compared with the high-throughput screening method. However, the scores of *in silico* screening did not seem to relate to IC_{50} values.

X-ray structural analysis of PfOMPDC in complex with HMOA

We attempted to crystallize *Pf*OMPDC with the 14 selected compounds, using both the soaking and co-crystallization methods. After many trials, we succeeded with the X-ray structural analysis of *Pf*OMPDC in complex with HMOA (compound 1 in Fig. 2), which exhibited an IC_{50} value of 170 μM. The crystal structure was refined at 2.1 Å resolution with R_{work} of 19.5% and R_{free} of 26.8% (Table I). The asymmetric unit contained a dimer of *Pf*OMPDC molecules, and superimposition of the two molecules showed a small root mean square deviation of 0.53 Å for the whole 318 C_α carbon atoms. This observation reveals similarity of the whole structure in the crystal packing (Fig. 3A).

The soaking time of the crystal into the HMOA-containing cryoprotectant solution was limited to 2 min to prevent the decay of the crystal. As a result, the electron density around carboxyl group of

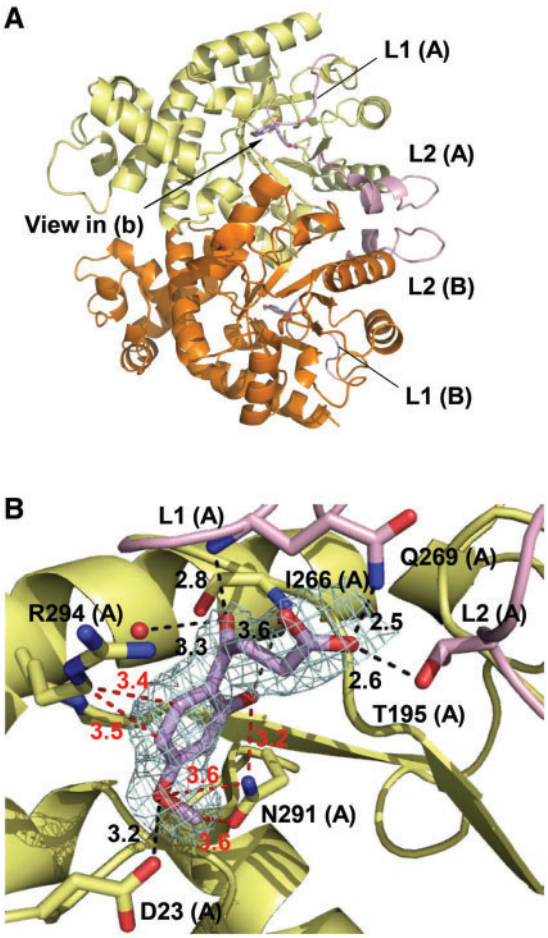

Fig. 3 The structure of *Pf*OMPDC in complex with HMOA. (**A**) Overall structure and (**B**) close-up view of the active site. The monomer molecules of *Pf*OMPDC are rendered in yellow and orange, and L1 and L2 loops are coloured pink. The inhibitor molecule of HMOA is coloured in light purple. Hydrogen bonds and hydrophobic interactions are displayed as black and red dashed lines, respectively. The $2F_o$-F_c map of the inhibitor is displayed in blue and contoured at 1.0σ. The figures were drawn with *PyMOL* (*27*).

HMOA was relatively weaker than around the aromatic ring of the inhibitor. The B-factor of the HMOA molecule was calculated to be 69.4 Å^2, which is relatively higher than the surrounding residues with an average B-factor of 28.3 Å^2. However, the electron density of the HMOA molecule was confirmed in each monomer in the asymmetric unit (Fig. 3B).

The HMOA complex showed that the carboxyl group of the inhibitor hydrogen bonded to both Gln269 in the L1 loop and Thr195 in the L2 loop. The carbonyl group of the inhibitor hydrogen bonded to both the main chain of Gln269 and a water molecule, and the hydroxyl group hydrogen bonded to the amide nitrogen atom of Ile266. There was a cation-π interaction between the aromatic ring of HMOA and the side chain of Arg294. van der Waals' interactions were also found between the hydroxyl group of HMOA and the N_δ nitrogen atom of Asn291, and between the methoxy group and the N_δ nitrogen and the O_δ oxygen atoms of Asn291. The

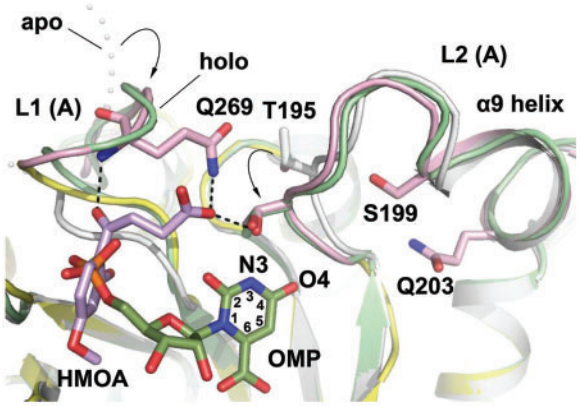

Fig. 4 Structural comparison of the HMOA-complex with the apo form and the OMP-complex. The apo form, the HMOA-complex and the holo form (the OMP-complex) are coloured white, pink and green, respectively. Although the L1 loop structure was disordered in the apo form, the loop was stabilized by a hydrogen bond between the carboxyl group of HMOA and Gln269. Thr195 dramatically rotated to interact with the same carboxyl group of the inhibitor along thereby inducing a structural change to the L2 loop on binding HMOA. This figure was drawn with *PyMOL* (*27*).

methoxy group also formed a hydrogen bond with Asp23.

Structural comparison of the HMOA complex with the apo form and the OMP or UMP-complex

Superimposition between the HMOA complex and the apo form (28) revealed that the binding of HMOA caused structural changes to the L1 and L2 loops (Fig. 4). Although the structure of the L1 loop was disordered in the apo form (PDB code 2ZA2), in the HMOA complex, this loop was stabilized by a hydrogen bond between the carboxyl group of the inhibitor and Gln269 in the L1 loop. In addition, Thr195 dramatically rotated to interact with the same carboxyl group of the inhibitor, inducing a conformational change to the L2 loop. The C_α carbon atom of Thr195 in the apo form had moved by 2.7 Å and the dihedral angle of the C_α-C_β bond in Thr195 had changed by 169° on binding of the inhibitor. In our previous work, the structure of the α9 helix (Ala200-Gln203) was completely unfolded on binding of OMP or UMP (28). In the HMOA complex, however, the structure of the α9 helix was not fully unfolded. The distance between the carbonyl oxygen atom of Ser199 and the amide nitrogen atom of Gln203 was measured to be 3.0 Å in the apo form, whereas in the HMOA complex, the distance was 3.6 Å. The same distance is 4.3 Å in the OMP or UMP complex. The structure of the α9 helix in the HMOA complex appears to be in an intermediate state between the apo and holo forms.

Among 14 inhibitor compounds, 11 compounds have a carboxyl group. Before solving the structure of the HMOA complex, the carboxyl group of HMOA was expected to bind in the active site where the phosphate group of OMP or UMP bound (28) by using the *in silico* screening methods (Supplementary Fig. 2). However, this carboxyl group interacted with both the L1 and L2 loops, and these loops are distal

from the phosphate bound region. Instead, the aromatic ring of the inhibitor bound in the phosphate binding site of the OMP or UMP complex. In the HMOA complex, there was no electron density around the region where the pyrimidine and the ribose rings were bound in the OMP or UMP complex. Instead, four water molecules occupied the space where the pyrimidine and the ribose rings bind. In the complex structure with OMP or UMP, the amide nitrogen atom and the hydroxyl group of Thr195 interact with O4 and N3 in the pyrimidine ring, respectively. Moreover, Thr145 in the α7 helix in the other protomer of the dimer stabilize the 2′-hydroxyl group in the ribose ring (28).

Compared with the OMP or UMP molecules, the lack of the pyrimidine and the ribose rings in the HMOA molecule may reduce the inhibition activity, therefore giving rise to the observed modest IC_{50} value of 170 μM. The *K*i value of UMP for *Pf*OMPDC was estimated to 210–250 μM (*10*, 29). UMP is the product of OMPDC and known to very weakly inhibit OMPDC. For further design and development of inhibitors against this enzyme, the HMOA molecule will be combined with pyrimidine and ribose ring moieties, thereby fully occupying the active site and stabilizing the inhibitor-protein complex. Structural analyses of the other 13 inhibitor-protein complexes are in progress. The completion of the structures of these complexes will advance fragment-based drug design and structure-based drug design against malaria.

Protein Data Bank accession numbers

The atomic coordinates and structure factors of *Pf*OMPDC in complex with HMOA have been deposited in the RCSB Protein Data Bank with the accession code 3VI2.

Supplementary Data

Supplementary Data are available at *JB* Online.

Acknowledgements

The authors express their appreciation to Dr. Keiji Tokuoka, Ms. Sachiyo Ito, Ms. Hitomi Furukawa-Matsuzaka, Mr. Takahiro Uchida, Mr. Noboru Nakano, Ms. Saki Konishi and Mr. Keishi Yamaguchi for their kind help in this study. We extend special thanks to Yoshiaki Mikami (Hitachi East Japan Solutions, Ltd.), Toshihiro Sakuma (NEC Informatec Systems, Ltd.), Masato Kitajima (Fujitsu Kyushu Systems, Ltd.), Yoshitada Fukuoka (Mitsui Knowledge Industry, Ltd.) and Ryuichi Shimizu (Urban Innovation Institute) for their support in inhibitor screening. The authors are grateful to the staff for their excellent support during data collection on the BL38B1 at SPring-8.

Funding

This work was supported by the Knowledge Cluster Initiative and in part by a Grant-in-Aid for Scientific Research (Nos. 16017260, 18350086, 22550152) from the Ministry of Education, Culture, Sports, Science and Technology of Japan (to T.I.).

Conflict of interest

None declared.

References

1. Guerin, P.J., Olliaro, P., Nosten, F., Druilhe, P., Laxminarayan, R., Binka, F., Kilama, W.L., Ford, N., and White, N.J. (2002) Malaria: current status of control, diagnosis, treatment, and a proposed agenda for research and development. *Lancet Infect. Dis.* **2**, 564–573
2. Attaran, A., Barnes, K.I., Curtis, C., d'Alessandro, U., Fanello, C.I., Galinski, M.R., Kokwaro, G., Looareesuwan, S., Makanga, M., Mutabingwa, T.K., Talisuna, A., Trape, J.F., and Watkins, W.M. (2004) WHO, the Global Fund, and medical malpractice in malaria treatment. *Lancet* **363**, 237–240
3. White, N.J. (2004) Antimalarial drug resistance. *J. Clin. Invest.* **113**, 1084–1092
4. Krungkrai, J., Cerami, A., and Henderson, G.B. (1990) Pyrimidine biosynthesis in parasitic protozoa: purification of a monofunctional dihydroorotase from Plasmodium berghei and Crithidia fasciculata. *Biochemistry*. **29**, 6270–6275
5. Jones, M.E. (1980) Pyrimidine nucleotide biosynthesis in animals: genes, enzymes, and regulation of UMP biosynthesis. *Annu. Rev. Biochem.* **49**, 253–279
6. Weber, G. (1983) Biochemical strategy of cancer cells and the design of chemotherapy: G. H. A. Clowes Memorial Lecture. *Cancer Res.* **43**, 3466–3492
7. Krungkrai, J., Prapunwatana, P., Wichitkul, C., Reungprapavut, S., Krungkrai, S.R., and Horii, T. (2003) Molecular biology and biochemistry of malarial parasite pyrimidine biosynthetic pathway. *Southeast Asian J. Trop. Med. Public Health* **34 (Suppl. 2)**, 32–43
8. Krungkrai, S.R., Aoki, S., Palacpac, N.M., Sato, D., Mitamura, T., Krungkrai, J., and Horii, T. (2004) Human malaria parasite orotate phosphoribosyltransferase: functional expression, characterization of kinetic reaction mechanism and inhibition profile. *Mol. Biochem. Parasitol.* **134**, 245–255
9. Krungkrai, S.R., Prapunwattana, P., Horii, T., and Krungkrai, J. (2004) Orotate phosphoribosyltransferase and orotidine 5′-monophosphate decarboxylase exist as multienzyme complex in human malaria parasite Plasmodium falciparum. *Biochem. Biophys. Res. Commun.* **318**, 1012–1018
10. Krungkrai, S.R., DelFraino, B.J., Smiley, J.A., Prapunwattana, P., Mitamura, T., Horii, T., and Krungkrai, J. (2005) A novel enzyme complex of orotate phosphoribosyltransferase and orotidine 5′-monophosphate decarboxylase in human malaria parasite Plasmodium falciparum: physical association, kinetics, and inhibition characterization. *Biochemistry*. **44**, 1643–1652
11. Livingstone, L.R. and Jones, M.E. (1987) The purification and preliminary characterization of UMP synthase from human placenta. *J. Biol. Chem.* **262**, 15726–15733
12. Suttle, D.P., Bugg, B.Y., Winkler, J.K., and Kanalas, J.J. (1988) Molecular cloning and nucleotide sequence for the complete coding region of human UMP synthase. *Proc. Natl. Acad. Sci. USA*. **85**, 1754–1758
13. Suchi, M., Mizuno, H., Kawai, Y., Tsuboi, T., Sumi, S., Okajima, K., Hodgson, M.E., Ogawa, H., and Wada, Y. (1997) Molecular cloning of the human UMP synthase gene and characterization of point mutations in two hereditary orotic aciduria families. *Am. J. Hum. Genet.* **60**, 525–539
14. Fukunishi, Y., Mikami, Y., Kubota, S., and Nakamura, H. (2006) Multiple target screening method for robust

and accurate in silico ligand screening. *J. Mol. Graph. Model.* **25**, 61–70
15. Fukunishi, Y., Mikami, Y., Takedomi, K., Yamanouchi, M., Shima, H., and Nakamura, H. (2006) Classification of chemical compounds by protein-compound docking for use in designing a focused library. *J. Med. Chem.* **49**, 523–533
16. Krungkrai, S.R., Tokuoka, K., Kusakari, Y., Inoue, T., Adachi, H., Matsumura, H., Takano, K., Murakami, S., Mori, Y., Kai, Y., Krungkrai, J., and Horii, T. (2006) Crystallization and preliminary crystallographic analysis of orotidine 5′-monophosphate decarboxylase from the human malaria parasite Plasmodium falciparum. *Acta. Crystallogr. Sect. F Struct. Biol. Cryst. Commun.* **62**, 542–545
17. Kollman, P.A., Massova, I., Reyes, C., Kuhn, B., Huo, S., Chong, L., Lee, M., Lee, T., Duan, Y., Wang, W., Donini, O., Cieplak, P., Srinivasan, J., Case, D.A., and Cheatham, T.E. 3rd (2000) Calculating structures and free energies of complex molecules: combining molecular mechanics and continuum models. *Acc. Chem. Res.* **33**, 889–897
18. Umezu, K., Amaya, T., Yoshimoto, A., and Tomita, K. (1971) Purification and properties of orotidine-5′-phosphate pyrophosphorylase and orotidine-5′-phosphate decarboxylase from baker's yeast. *J. Biochem.* **70**, 249–262
19. Otwinowski, Z. and Minor, W. (1997) Processing of X-ray diffraction data collected in oscillation mode. *Methods Enzymol.* **276**, 307–326
20. Vagin, A. and Teplyakov, A. (1997) MOLREP: an Automated Program for Molecular Replacement. *J. Appl. Cryst.* **30**, 1022–1025
21. Collaborative Computational Project, Number 4. *Acta. Cryst. D Biol. Crystallogr.* **D50**, 760–763
22. Cowtan, K. (1994) 'dm': an automated procedure for phase improvement by density modification. *Joint CCP4 and ESF-EACBM Newsletter on Protein Crystallogr.* **31**, 34–38
23. Adams, P.D., Pannu, N.S., Read, R.J., and Brunger, A.T. (1997) Cross-validated maximum likelihood enhances crystallographic simulated annealing refinement. *Proc. Natl. Acad. Sci. USA.* **94**, 5018–5023
24. Murshudov, G.N., Vagin, A.A., and Dodson, E.J. (1997) Refinement of macromolecular structures by the maximum-likelihood method. *Acta. Crystallogr. D Biol. Crystallogr.* **53**, 240–255
25. Emsley, P. and Cowtan, K. (2004) Coot: model-building tools for molecular graphics. *Acta. Crystallogr. D Biol. Crystallogr.* **60**, 2126–2132
26. Davies, J.W., Glick, M., and Jenkins, J.L. (2006) Streamlining lead discovery by aligning in silico and high-throughput screening. *Curr. Opin. Chem. Biol.* **10**, 343–351
27. DeLano, W.L. (2005) The case for open-source software in drug discovery. *Drug Discov. Today.* **10**, 213–217
28. Poduch, E., Wei, L., Pai, E.F., and Kotra, L.P. (2008) Structural diversity and plasticity associated with nucleotides targeting orotidine monophosphate decarboxylase. *J. Med. Chem.* **51**, 432–438
29. Tokuoka, K., Kusakari, Y., Krungkrai, S.R., Matsumura, H., Kai, Y., Krungkrai, J., Horii, T., and Inoue, T. (2008) Structural basis for the decarboxylation of orotidine 5′-monophosphate (OMP) by Plasmodium falciparum OMP decarboxylase. *J. Biochem.* **143**, 69–78